Editors' Suggestion

Magnetoconduction in the Correlated Semiconductor FeSi in Ultrastrong Magnetic Fields up to a Semiconductor-to-Metal Transition

D. Nakamura, * Y. H. Matsuda, A. Ikeda, A. Miyake, M. Tokunaga, and S. Takeyama †
The Institute for Solid State Physics, The University of Tokyo, Kashiwa, Chiba 277-8581, Japan

T. Kanomata
Research Institute for Engineering and Technology, Tohoku Gakuin University, Tagajo, Miyagi 985-8537, Japan

(Received 7 May 2021; revised 9 July 2021; accepted 2 September 2021; published 6 October 2021)

Magnetoresistance of the correlated narrow-gap semiconductor FeSi was investigated by the radio frequency self-resonant spiral coil technique in magnetic fields up to 500 T, which is supplied by an electromagnetic flux compression megagauss generator. Semiconductor-to-metal transition accomplishes around 270 T observed as a sharp kink in the magnetoresistance, which implies the closing of the hybridization gap by the Zeeman shift of band edges. In the temperature-magnetic field phase diagram, the semiconductor-metal transition field is found to be almost independent of temperature, which is in contrast to a characteristic magnetic field associated with the hopping magnetoconduction in the in-gap localized states, exhibiting a notable temperature dependence.

DOI: 10.1103/PhysRevLett.127.156601

Narrow-gap semiconductor alloys have been widely recognized as a prototypical material used in far-infrared optoelectronics, some of which have yet another intriguing aspect as a strongly correlated electron system. A typical example is the Kondo semiconductor, where the conduction and localized electrons form a nonmagnetic Kondo singlet state as a consequence of the strong electron correlation.

Iron monosilicide FeSi, which exhibits mysterious transport, thermoelectric, and magnetic properties followed by semiconductor-metal (S-M) transition, similar to those of the Kondo semiconductor, has been a target of intense and long-standing studies for more than half a century [1]. A trend of recent studies [2,3] is to regard FeSi as a correlated narrow-gap semiconductor without the formation of the Kondo singlet. In the band structure calculation [3], formation of a hybridization gap (termed in this Letter as "h gap") is predicted as a result of the orbital hybridization between Fe $3d$ and Si $2p$ bands. The presence of a sharp peak across the energy gap in the density-of-state calculation [4] is indicative of the underlying significance of a correlation effect.

On the other hand, the h gap energy determined from low-temperature experiments differs from one report to the others (50–70 meV) [1,5–15], and they are insufficient to support existing theoretical models under review. In addition, size-dependent electrical resistivity characteristic of a topological surface state recently observed below 19 K [8] suggests a potential difficulty in extracting the bulk band structure especially at low temperatures by means of surface-sensitive measurements such as the angle-resolved photoemission spectroscopy.

Application of an external ultrastrong magnetic field to these interacting yet puzzling electrons in FeSi is expected to open an avenue for exploring the band structure details in a highly correlated electron system. When the h gap is narrow, an energy shift of the electronic band by the spin Zeeman effect should have driven a change in the magnetic and transport properties. Some calculations have predicted the existence of the metamagnetic and associated S-M transition at 170 T [16,17], 354 T, and 700 T [18]. However, the calculated transition field sensitively depends on the gap magnitude, a fact that obscures a conclusive prediction. In the late 1990s, the magnetization and the radio frequency electrical resistivity measurements were conducted in magnetic fields of up to 450 T [19,20], where the chemical explosive flux compression technique was used to generate ultrahigh magnetic fields [21]. Although an anomalous increase in the electrical conductivity was detected around 355 T, the transition point and the details of conductivity evolution are yet indistinct. In order to open insights into the issue mentioned above, precision and reliable transport measurement techniques have been expected to be developed in such an extreme environment of ultrastrong magnetic fields.

Recent progress and developments in the electromagnetic flux compression (EMFC) techniques have achieved a remarkable capability to produce 1000-T-class highly controllable magnetic fields, allowing precision physical property measurements [22]. In addition, a radio frequency self-resonant spiral coil technique recently developed in an environment of exploding short-pulse magnets has enabled us to conduct a sensitive ac conductivity measurement [23]. All the instruments and measurement techniques needed in

FeSi are ready for a recurrence of searches for magnetoresistance behavior in ultrastrong magnetic fields. In this Letter, the magnetic field of up to 500 T is applied to ac conductivity measurements of FeSi, from which the S-M phase diagram was accomplished.

A single crystal of FeSi was fabricated by the Czochralski technique. The detail of the sample quality was described in Ref. [10], where FeSi samples were taken from the same ingot as samples used in this Letter. The temperature dependent magnetic susceptibility obtained by the Magnetic Properties Measurement System (Quantum Design) was confirmed to be quantitatively the same as that of Koyama *et al.* [10]. A FeSi bulk crystal was cut into the dimension of $2 \times 1.2 \times 0.3$ mm^3, and then the gold electrode was evaporated by the sputtering machine. The temperature dependence of dc electrical resistivity [$\rho_{dc}(B = 0)$] was measured by the Physical Properties Measurement System (PPMS, Quantum Design; 10 Hz ac mode).

Magnetic fields up to 500 T were produced by a microsecond pulse mode with exploding destructive operation, the EMFC technique [22]. The electrical resistivity was measured by the radio frequency contactless self-resonant spiral coil technique [23]. A measurement sample with a typical dimension of $1 \times 1 \times 0.05$ mm^3 was glued on the probe coil (self-resonant spiral coil), to which the radio frequency (rf) voltage tuned around 700 MHz was applied. The returned signal from the probe coil (V_{rf}) was converted to the electrical resistivity (ρ_{ac}), via a calibration curve of V_{rf} with respect to ρ_{dc}. Details of the signal processing are described in Ref. [23]. The (100) plane of a sample with the probe coil was set parallel to the magnetic field axis to avoid Joule heating induced by the eddy current subjected to an extremely short and intense pulse field ($dB/dt \sim 5 \times 10^7$ T/s). Temperature is monitored by an Au(Fe)-Chromel thermocouple or a RuO_2 resistor chip set adjacent to the sample, and is measured just before an ignition of pulse magnetic field and recorded as initial temperature, T_{init}. The experimental details are presented in the Supplemental Material [24].

The result of the PPMS measurement in the absence of the magnetic field is shown in Fig. 1. The temperature dependence of $\rho_{dc}(B = 0)$ is plotted against the reverse temperature ($1/T$). Above $T^* = 80$ K (shaded with red background), an h gap (Δ) of 54 meV was evaluated from the slope of Arrhenius plot above T^* ($\rho_{bulk} \propto \exp[\Delta/2k_BT]$).

As is noticed in Fig. 1, the Arrhenius plot deviates from a single straight line at temperatures below T^*, indicating that the carrier dynamics shifts to a nonthermal activation type inside the band gap. Among various conduction mechanisms at low temperatures, ρ_{dc} below T^* can be interpreted by the variable range hopping (VRH) of localized carriers in the in-gap states. In the Mott-type VRH without the electron correlation, $\rho(T)$ is described as

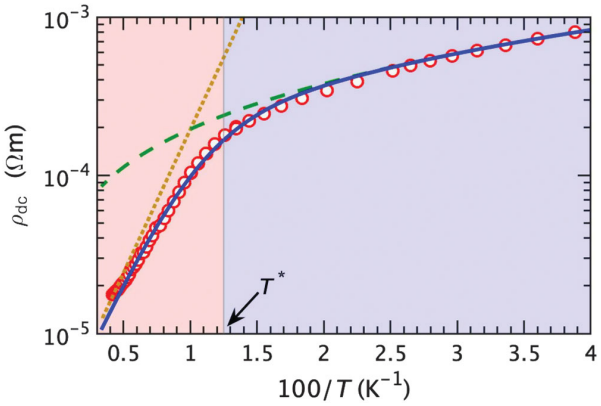

FIG. 1. Temperature dependence of dc electrical resistivity measured by PPMS. Two regions of temperature range are divided by a boundary line ($T^* = 80$ K) on the basis of each transport mechanism. The solid curve is a fitting result of ρ_{dc}. An intrinsic band gap and in-gap components of the fitting curve are shown by a dotted and a dashed line, respectively.

$\rho_{Mott} = \rho_0 \exp[(T_0/T)^{1/4}]$ [29], where ρ_0 and T_0 are constant. As shown in Fig. 1, ρ_{dc} in the whole range of temperature is well reproduced by a fitting curve $\rho_{fit}^{-1} = \rho_{Mott}^{-1} + \rho_{bulk}^{-1}$ (solid curve), with a set of parameters, $\Delta = 72$ meV and $T_0 = 1.48$ eV. A magnitude similar to T_0 was reported by Takagi *et al.* ($T_0 = 1.42$ eV [30]). This result implies that an electrical conduction at higher temperatures is dominated by the thermally activated carriers across the gap, whereas at low-temperatures below T^* the VRH conduction takes place in the in-gap localized states.

The existence of the midgap states has been suggested by previous studies [31–34]. Most recently, Fang *et al.* investigated $\rho(T)$ of a high-quality low-carrier sample, and the energy scale of 35 meV was found from temperature dependences of the resistance between 54 K and 30 K [8], which is almost half of the h gap. However, the origin of the midgap states in FeSi remains a subject of speculation. Several scenarios can be considered based on the effect stemming from the strong electron correlation [35,36], spin polaron [32], and phonon-related excitation [37–42], whose issue is out of the scope of the present work.

The result of ac conductivity measurement under the magnetic field up to 420 T at $T_{init} = 53$ K is shown in Fig. 2(a), where the time evolution of high-frequency probe signal (V_{rf}) from the self-resonant spiral coil is displayed (upper panel) alongside that of the pulse magnetic field (lower panel). The amplitude of V_{rf} increases with the magnetic field, and saturates at 275 T. $B(t)$ and $V_{rf}(t)$ measured at 29 K and 6 K are shown in the Supplemental Material [24].

In Fig. 2(b), $\rho_{ac}(B)$ converted from V_{rf} at $T_{init} = 53$ K, 29 K, and 6 K are presented. The open circles are $\rho_{dc}(B = 0)$ drawn from Fig. 1. The anomalous fields (B_{sh}, $B_{S\text{-}M'}$, and $B_{S\text{-}M}$, defined later on) in $\rho_{ac}(B)$ are pointed by the arrows. At 53 K, a sparse positive

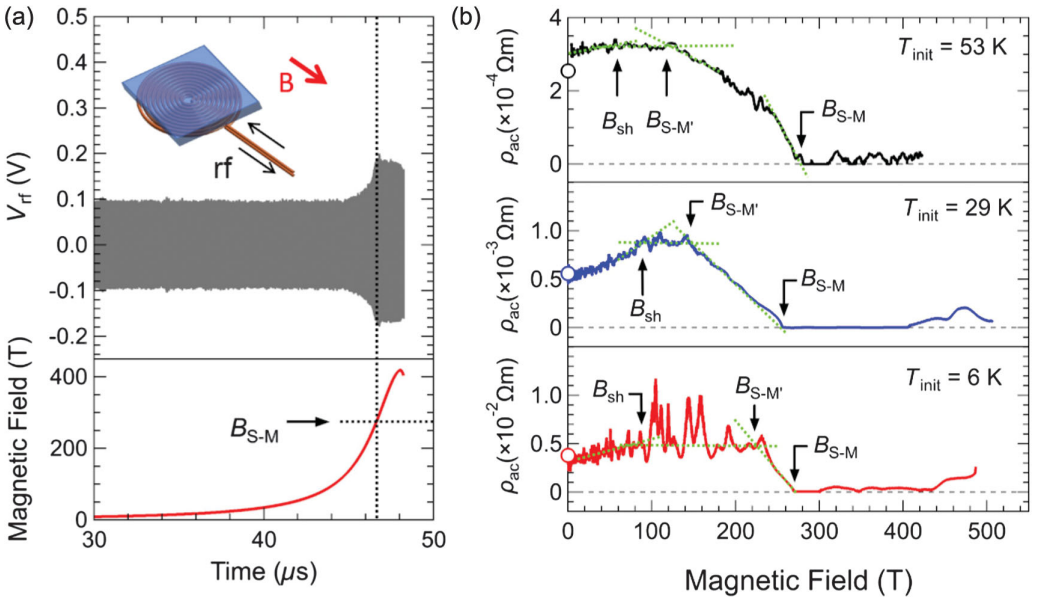

FIG. 2. Results of the high-field experiments. (a) Time evolution of V_{rf} (upper panel) and a pulsed magnetic field (lower panel) at 53 K. The inset is a schematic configuration of an FeSi sample and probe coil. (b) Magnetic field dependence of the electrical resistivity at 53 K, 29 K, and 6 K. Characteristic magnetic field intensities B_{sh}, $B_{S\text{-}M'}$, and $B_{S\text{-}M}$ are pointed by arrows, which are determined by an intersection of light-green dotted tangential lines.

magnetoresistance continues until a shoulderlike structure at 60 T (B_{sh}). Then, $\rho_{ac}(B)$ shows a gradual decrease starting approximately above 118 T ($B_{S\text{-}M'}$). We found a sudden drop in ρ_{ac} with a clear kink at 275 T ($B_{S\text{-}M}$), above which $\rho_{ac}(B)$ saturates and approaches approximately zero. Upon decreasing temperature from 53 K to 6 K, a positive magnetoresistance below B_{sh} and a saturating behavior up to $B_{S\text{-}M'}$ become more pronounced due to a significant increase of the magnetoresistance ratio. A positive magnetoresistance has also been reported in the previous high-field study up to 35 T [9].

Note that in Fig. 1 $\rho_{dc}(T < T^*, B = 0)$ has been well explained by the VRH mechanism on the midgap localized states. Accordingly, at low temperatures below $T < T^*$, the magnetoresistance up to the magnetic field $B_{S\text{-}M'}$ can also be characterized by the VRH conduction involving the midgap states. Quite similarly to our observation up to $B_{S\text{-}M'}$ in Fig. 2(b), positive magnetoresistance with a linear dependence on a magnetic field and saturation above a certain magnetic field (corresponding to B_{sh}) were found by the calculation based on the VRH theory taking account of the intrastate correlation, which was revealed by Kurobe and Kawamura [43].

Summarizing the above results, the temperature- and magnetic-field-dependent electronic energy band is schematically illustrated in Fig. 3. (a) At a zero magnetic field, the Arrhenius-type thermal activation took place over the h gap above T^*, and changed to the VRH-type conduction in the midgap states at lower temperatures. (b) By increasing the magnetic fields up to $B_{S\text{-}M'}$, the conduction involving the midgap states remains dominant.

As shown in Fig. 3(c), $\Delta(B)$ becomes sufficiently small above $B_{S\text{-}M'}$ due to the substantial Zeeman shift of band edges, which makes the Arrhenius-type thermal activation dominant again. Further suppression of the h gap with an increasing magnetic field assists the thermal activation of electrons and induces a gradual decrease in ρ_{ac} between $B_{S\text{-}M'}$ and $B_{S\text{-}M}$. Then, the conduction and the valence band edges across the h gap begin to overlap each other, which induces an abrupt drop in ρ_{ac} just below $B_{S\text{-}M}$. Accordingly, $B_{S\text{-}M}$ should be regarded as a magnetic field intensity where the S-M transition is accomplished as shown in Fig. 3(d). A recurrent increase in $\rho_{ac}(B)$ observed above 400 T at 29K

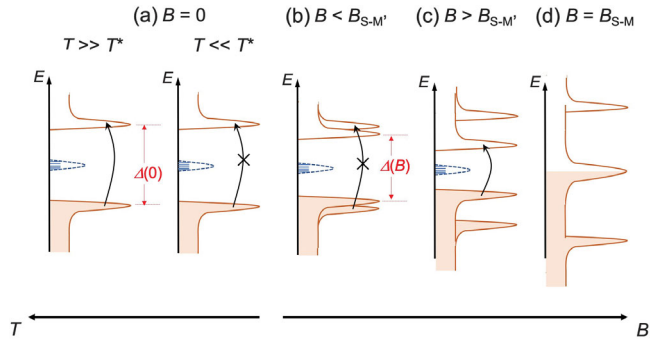

FIG. 3. Schematic illustration of the electronic energy bands in a characteristic range of temperatures and magnetic fields, (a) to (d), in accordance with different events of each transport phenomenon. The blue energy levels indicate the midgap states, which dominate the electrical transport phenomenon below $B_{S\text{-}M'}$ and temperature below T^*. Symbol × represents an inactivated transition over the hybridization gap Δ.

and 6 K could be simply an artifact signal noise or could be most possibly caused by a metamagnetictype magnetization increase associated with the S-M transition [16–18], which could be unintentionally detected by the probe coil.

The magnitude of the h gap at $B = 0$ is also estimated from $B_{\text{S-M}}$, as follows. The Zeeman shift of the conduction and the valence band edges, $E_{c,v}(B) = E_{c,v}(B = 0) \pm g\mu_B|S|B$, where g is the g factor, μ_B is the Bohr magneton, and S is the spin quantum number, can close the h gap. The corresponding energy shift at $B_{\text{S-M}}$ $(T = 53\ \text{K}) = 275$ T is evaluated as $2g\mu_B|S|B_{\text{S-M}} = 64$ meV, if $(S, g) = (1, 2)$ referred from the recent theory [44] is adopted. This value is slightly smaller but compatible with a value of the h gap (72 meV) deduced from Fig. 1, and also consistent with the values 50–70 meV observed in previous reports [1,5–15].

Magnetic field dependence of the h gap $\Delta(B)$ can be evaluated in a similar manner as in Fig. 1, provided that the Arrhenius plot is yielded for $\rho_{\text{ac}}(T)$ at a given magnetic field, which is possible to construct at a magnetic field $B = B_{\text{S-M}'}$, using the value $\rho_{\text{ac}}(T, B = B_{\text{S-M}'})$ as described in detail in the Supplemental Material [24]. We found that $\Delta(B)$ gradually decreases with an increasing magnetic field as is seen in Fig. S3 of the Supplemental Material, which is consistent with the collapse of the h gap by the spin Zeeman effect as schematically illustrated in Fig. 3.

B_{sh}, $B_{\text{S-M}'}$ and $B_{\text{S-M}}$ are plotted in the T–B phase diagram by open circles and squares in Fig. 4. During an extremely short duration time of the pulse magnetic field of a microsecond order, thermal dissipation to the surrounding environment is hardly expected around the sample, which is exposed to a temperature increase from the Joule heating during the pulse, termed as the sample temperature,

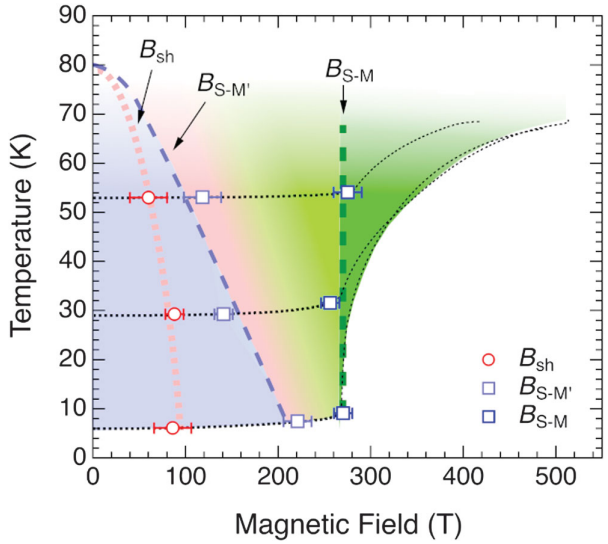

FIG. 4. T–B phase diagram of electronic conduction. Thin black dotted lines show the sample temperatures evaluated from calculated Joule heating. The bold dotted (dashed) curves are guidelines of phase boundaries derived from characteristic magnetic field B_{sh} ($B_{\text{S-M}'}$ and $B_{\text{S-M}}$).

$T_{\text{samp}} = T_{\text{init}} + \delta T(B)$. The thin dotted lines in Fig. 4 are the sample temperatures $T_{\text{samp}}[B(t)]$ evaluated by calculating the Joule heating in each experiment assuming an adiabatic condition (see Supplemental Material). The sample temperature gradually develops from T_{init}, and shows an abrupt increase above $B_{\text{S-M}}$ due to the field-induced metallic conductivity. B_{sh} and $B_{\text{S-M}'}$ disappear around $T^* = 80$ K as guided by (red) dotted and (pale blue) dashed curves, respectively. On the other hand, $B_{\text{S-M}}$ stays still at 267 ± 10 T at temperatures between 53 K and 6 K (the bold dashed line). It is to be noted that the h gap has been reported to be almost independent on temperatures below ~100 K [14,45], which is consistent with temperature-independent $B_{\text{S-M}}$ obtained in this work. As distinguished by different background colors in Fig. 4, characteristic magnetic fields ($B_{\text{S-M}'}$ and $B_{\text{S-M}}$) separate the magnetic field regimes of different types of electronic conduction, which are illustrated in Figs. 3(b)–3(d).

To sum up, the magnetoresistance of correlated narrow-gap magnetic semiconductor FeSi was investigated in ultrastrong magnetic fields up to 500 T, which is supplied by the electromagnetic flux compression technique. On increasing magnetic fields, four distinct phase changes were successively observed, firstly positive magnetoresistance, and then its saturation area followed by a slow decrease of the resistance up to a well-defined S-M transition at 267 T. The S-M transition is well explained by a band gap squashed into a zero-gap state that is compressed by the giant Zeeman effect induced by ultrastrong magnetic fields.

D. N. acknowledges partial financial support from JSPS KAKENHI Grant No. JP19K03710. The authors are obliged to T. Tomita and R. Note for helping with the synthesis of a FeSi crystal, and to H. Sawabe for his diligent technical support.

*daisuke.nakamura.rg@riken.jp
Present address: RIKEN Center for Emergent Matter Science (CEMS), 2-1 Hirosawa, Wako 351-0198, JAPAN.
†takeyama@issp.u-tokyo.ac.jp

[1] R. Wolfe, J. H. Wernick, and S. E. Haszko, Thermoelectric properties of FeSi, Phys. Lett. **19**, 449 (1965).
[2] J. M. Tomczak, K. Haule, and G. Kotliar, Signatures of electronic correlations in iron silicide, Proc. Natl. Acad. Sci. U.S.A. **109**, 3243 (2012).
[3] J. M. Tomczak, Thermoelectricity in correlated narrow-gap semiconductors, J. Phys.: Condens. Matter **30**, 183001 (2018).
[4] C. Fu, M. P. C. M. Krijn, and S. Doniach, Electronic structure and optical properties of FeSi, a strongly correlated insulator, Phys. Rev. B **49**, 2219 (1994).
[5] Z. Schlesinger, Z. Fisk, H. Zhang, M. B. Maple, J. DiTusa, and G. Aeppli, Unconventional Charge Gap Formation in FeSi, Phys. Rev. Lett. **71**, 1748 (1993).
[6] V. Jaccarino, G. K. Wertheim, J. H. Wernick, L. R. Walker, and S. Arajs, Paramagnetic excited state of FeSi, Phys. Rev. **160**, 476 (1967).

[7] S. Paschen, E. Felder, M. A. Chernikov, L. Degiorgi, H. Schwer, H. R. Ott, D. P. Young, J. L. Sarrao, and Z. Fisk, Low-temperature transport, thermodynamic, and optical properties of FeSi, Phys. Rev. B **56**, 12916 (1997).
[8] Y. Fang, S. Ran, W. Xie, S. Wang, Y. S. Meng, and M. B. Maple, Evidence for a conducting surface ground state in high-quality single crystalline FeSi, Proc. Natl. Acad. Sci. U.S.A. **115**, 8558 (2018).
[9] K. G. Lisunov, E. K. Arushanov, Ch. Kloc, J. Broto, J. Leotin, H. Rokoto, M. Respaud, and E. Bucher, Conductivity and magnetoresistance of FeSi in the Anderson-localized regime, Physica (Amsterdam) **229B**, 37 (1996).
[10] K. Koyama, T. Goto, T. Kanomata, and R. Note, Precise magnetization measurements of single-crystalline FeSi under high pressure, J. Phys. Soc. Jpn. **68**, 1693 (1999).
[11] H. Ohta, T. Arioka, Y. Yamamoto, S. Mitsudo, T. Hamamoto, M. Motokawa, Y. Yamaguchi, and E. Kulatov, Magnetoresistance measurements of FeSi under high magnetic field, Physica (Amsterdam) **237–238B**, 463 (1997).
[12] N. E. Sluchanko, V. V. Glushkov, S. V. Demishev, M. V. Kondrin, K. M. Petukhov, A A. Pronin, N. A. Samarin, Y. Bruynseraede, V. V. Moshchalkov, and A. A. Menovsky, Low-temperature anomalies of the Hall coefficient in FeSi, JETP Lett. **68**, 817 (1998).
[13] P. Samuely, P. Szabó, M. Mihalik, N. Hudáková, and A. A. Menovsky, Gap formation in Kondo insulator FeSi: Point contact spectroscopy, Physica (Amsterdam) **218B**, 185 (1996).
[14] M. Fäth, J. Aarts, A. A. Menovsky, G. J. Nieuwenhuys, and J. A. Mydosh, Tunneling spectroscopy on the correlation effects in FeSi, Phys. Rev. B **58**, 15483 (1998).
[15] J. F. DiTusa, K. Friemelt, E. Bucher, G. Aeppli, and A. P. Ramirez, Heavy fermion metal–Kondo insulator transition in $FeSi_{1-x}Al_x$, Phys. Rev. B **58**, 10288 (1998).
[16] V. I. Anisimov, S. Y. Ezhov, I. S. Elfimov, I. V. Solovyev, and T. M. Rice, Singlet Semiconductor to Ferromagnetic Metal Transition in FeSi, Phys. Rev. Lett. **76**, 1735 (1996).
[17] E. Kulatov and H. Ohta, Field-induced itinerant metamagnetism in iron monosilicide, J. Phys. Soc. Jpn. **66**, 2386 (1997).
[18] H. Yamada, K. Terao, H. Ohta, T. Arioka, and E. Kulatov, Electronic structure and the metamagnetic transition of FeSi at extremely high magnetic fields, J. Phys.: Condens. Matter **11**, L309 (1999).
[19] Y. B. Kudasov *et al.*, Semiconductor-metal transition in FeSi in ultrahigh magnetic fields up to 450 T, J. Exp. Theor. Phys. Lett. **68**, 350 (1998).
[20] Y. B. Kudasov *et al.*, Semiconductor-metal transition in FeSi in an ultrahigh magnetic field, J. Exp. Theor. Phys. **89**, 960 (1999).
[21] C. M. Fowler, W. B. Garn, and R. S. Caird, Production of very high magnetic fields by implosion, J. Appl. Phys. **31**, 588 (1960).
[22] D. Nakamura, A. Ikeda, H. Sawabe, Y. H. Matsuda, and S. Takeyama, Record indoor magnetic field of 1200 T generated by electromagnetic flux-compression, Rev. Sci. Instrum. **89**, 095106 (2018).
[23] D. Nakamura, M. M. Altarawneh, and S. Takeyama, Radio frequency self-resonant coil for contactless AC-conductivity in 100 T class ultra-strong pulse magnetic fields, Meas. Sci. Technol. **29**, 035901 (2018).
[24] See Supplemental Material at http://link.aps.org/supplemental/10.1103/PhysRevLett.127.156601 for Joule heating effect induced by a pulsed magnetic field, additional data of high-field magnetoconduction measurements, estimation of magnetic field dependence of the hybridization gap, comparison with previous high-field study and details of measurement setup, which includes Refs. [1,19,20,25–28].
[25] J. Acker, K. Bohmhammel, G. J. K. van den Berg, J. C. van Miltenburg, and Ch. Kloc, Thermodynamic properties of iron silicides FeSi and α-$FeSi_2$, J. Chem. Thermodyn. **31**, 1523 (1999).
[26] P. Sun, B. Wei, D. Menzel, and F. Steglich, Resonant charge relaxation as a likely source of the enhanced thermopower in FeSi, Phys. Rev. B **90**, 245146 (2014).
[27] D. Nakamura, T. Adachi, K. Omori, Y. Koike, and S. Takeyama, Pauli-limit upper critical field of high-temperature superconductor $La_{1.84}Sr_{0.16}CuO_4$, Sci. Rep. **9**, 16949 (2019).
[28] D. Nakamura, H. Sawabe, Y. H. Matsuda, and S. Takeyama, Precise measurement of a magnetic field generated by the electromagnetic flux compression technique, Rev. Sci. Instrum. **84**, 044702 (2013).
[29] N. F. Mott, Conduction in non-crystalline materials, Philos. Mag. **19**, 835 (1969).
[30] S. Takagi, H. Yasuoka, S. Ogawa, and J. H. Wernick, ^{29}Si NMR studies of an "unusual" paramagnet FeSi –Anderson localized state model–, J. Phys. Soc. Jpn. **50**, 2539 (1981).
[31] L. Degiorgi, M. B. Hunt, H. R. Ott, M. Dressel, B. J. Feenstra, G. Grüner, Z. Fisk, and P. Canfield, Optical evidence of Anderson-Mott localization in FeSi, Europhys. Lett. **28**, 341 (1994).
[32] N. E. Sluchanko, V. V. Glushkov, S. V. Demishev, M. V. Kondrin, K. M. Petukhov, N. A. Samarin, V. V. Moshchalkov, and A. A. Menovsky, Thermopower in the regime of strong Hubbard correlations in FeSi, Europhys. Lett. **51**, 557 (2000).
[33] N. E. Sluchanko, V. V. Glushkov, S. V. Demishev, A. A. Menovsky, L. Weckhuysen, and V. V. Moshchalkov, Crossover in magnetic properties of FeSi, Phys. Rev. B **65**, 064404 (2002).
[34] V. V. Glushkov, B. P. Gorshunov, E. S. Zhukova, S. V. Demishev, A. A. Pronin, N. E. Sluchanko, S. Kaiser, and M. Dressel, Spin excitations of the correlated semiconductor FeSi probed by THz radiation, Phys. Rev. B **84**, 073108 (2011).
[35] X. Y. Zhang, M. J. Rozenberg, and G. Kotliar, Mott Transition in the $d = \infty$ Hubbard Model at Zero Temperature, Phys. Rev. Lett. **70**, 1666 (1993).
[36] M. J. Rozenberg, G. Kotliar, and H. Kajueter, Transfer of spectral weight in spectroscopies of correlated electron systems, Phys. Rev. B **54**, 8452 (1996).
[37] T. Jarlborg, Electronic structure and properties of pure and doped ϵ-FeSi from *ab initio* local-density theory, Phys. Rev. B **59**, 15002 (1999).
[38] T. Jarlborg, Importance of thermal disorder and electronic occupation for temperature dependence of optical conductivity in FeSi and MnSi, Phys. Rev. B **76**, 205105 (2007).

[39] O. Delaire, K. Marty, M. B. Stone, P. R. C. Kent, M. S. Lucas, D. L. Abernathy, D. Mandrus, and B. C. Sales, Phonon softening and metallization of a narrow-gap semiconductor by thermal disorder, Proc. Natl. Acad. Sci. U.S.A. **108**, 4725 (2011).

[40] O. Delaire, I. I. Al-Qasir, J. Ma, A. M. dos Santos, B. C. Sales, L. Mauger, M. B. Stone, D. L. Abernathy, Y. Xiao, and M. Somayazulu, Effects of temperature and pressure on phonons in $FeSi_{1-x}Al_x$, Phys. Rev. B **87**, 184304 (2013).

[41] S. Krannich *et al.*, Magnetic moments induce strong phonon renormalization in FeSi, Nat. Commun. **6**, 8961 (2015).

[42] P. P. Parshin, A. I. Chumakov, P. A. Alekseev, K. S. Nemkovski, L. Dubrovinskii, A. Kantor, J. Perßon, and R. Rüffer, Peculiarities of FeSi phonon spectrum induced by a change of atomic volume, J. Exp. Theor. Phys. **123**, 1073 (2016).

[43] A. Kurobe and H. Kamimura, Correlation effects on variable range hopping conduction and the magnetoresistance, J. Phys. Soc. Jpn. **51**, 1904 (1982).

[44] J. M. Tomczak, K. Haule, and G. Kotliar, Thermopower of the correlated narrow gap semiconductor FeSi and comparison to RuSi, in *New Materials for Thermoelectric Applications: Theory and Experiment*, edited by V. Zlatic and A. Hewson (Springer Netherlands, Dordrecht, 2013), p. 45, https://dx.doi.org/10.1007/978-94-007-4984-9.

[45] M. Arita *et al.*, Angle-resolved photoemission study of the strongly correlated semiconductor FeSi, Phys. Rev. B **77**, 205117 (2008).